Accepted Manuscript

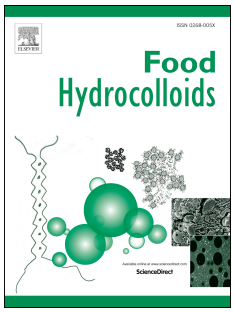

Improved emulsion stability and modified nutrient release by structuring O/W emulsions using konjac glucomannan

Wei Lu, Baodong Zheng, Song Miao

PII: S0268-005X(17)31913-6

DOI: 10.1016/j.foodhyd.2018.02.034

Reference: FOOHYD 4293

To appear in: *Food Hydrocolloids*

Received Date: 13 November 2017

Revised Date: 24 January 2018

Accepted Date: 19 February 2018

Please cite this article as: Lu, W., Zheng, B., Miao, S., Improved emulsion stability and modified nutrient release by structuring O/W emulsions using konjac glucomannan, *Food Hydrocolloids* (2018), doi: 10.1016/j.foodhyd.2018.02.034.

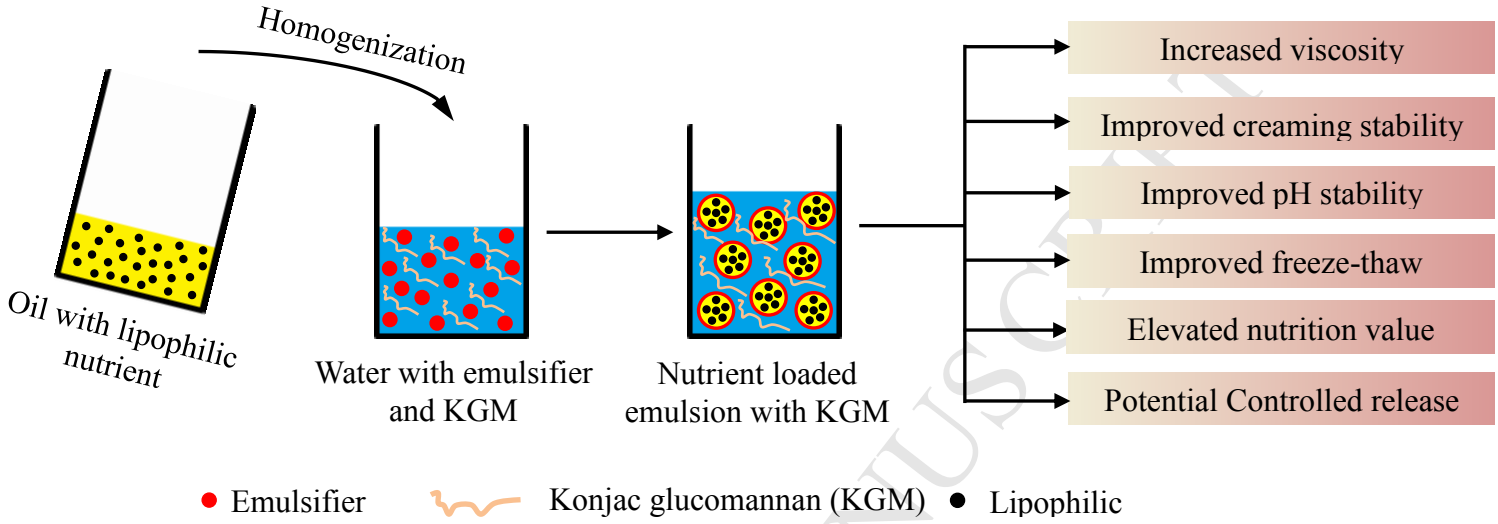

Improved emulsion stability and modified nutrient release by structuring O/W emulsions using konjac glucomannan

Wei Lu[1, 2], Baodong Zheng[3], Song Miao[1,3*]

[1]*Teagasc Food Research Centre, Moorepark, Fermoy, Cork, Ireland*

[2]*School of Food and Nutritional Sciences, University College Cork, Cork, Ireland*

[3]*China-Ireland International Cooperation Center for Food Material Science and Structure Design, Fujian Agriculture and Forestry University, Fuzhou, China*

[*]Corresponding author

Tel: +353 (0) 25 42468

Fax: +353 (0) 25 42340

E-mail: song.miao@teagasc.ie

Abstract

Functional konjac glucomannan (KGM) was used to structure the water phase of O/W emulsions containing a lipophilic bioactive compound (β-carotene). KGM greatly increased the viscosity of the water phase and thus the viscosity of final emulsions. Results of Fourier-transform infrared spectroscopy (FT-IR) showed that there is no significant non-covalent interaction between KGM and whey proteins in the water phase. KGM significantly improved the creaming and pH stability of whey-protein-stabilized emulsions (p<0.05), and significantly decreased the oiling-off of emulsions during freeze-thaw test. Emulsions with or without KGM all had good thermal stability at 80 °C. Microscopy observations indicated obvious aggregation of free proteins and oil droplets in gastric phase and an enzymatic-induced break-down of droplets, mainly in the intestinal phase of the simulated gastrointestinal tract (GIT). Emulsions with KGM-structured water phase showed a lower final release rate of encapsulated β-carotene than emulsion without KGM (p<0.05), and the release rate decreased with the increasing KGM content. The findings of this study contribute to a better understanding of the influence of the water phase on the release of encapsulated compounds from emulsions, and make it possible to achieve controlled release of encapsulated compounds, and/or to deliver multiple functional ingredients in one carrier by structuring the water phase of emulsion with functional polymers.

Keywords: emulsion, water phase, konjac glucomannan, stability, release

1. Introduction

There has been a growing interest in the utilization of emulsions as the carriers for the encapsulation, protection and delivery of lipophilic functional nutrients. Many emulsion-based carriers have been successfully developed to protectively deliver a variety of bioactive molecules, such as carotenoids (Lu et al., 2016; Lu, Kelly, & Miao, 2017b), fatty acids (Karthik & Anandharamakrishnan, 2016), polyphenols (Lu, Kelly, & Miao, 2016), peptides (Niu, Conejos-Sanchez, Griffin, O'Driscoll, & Alonso, 2016) and novel drugs (Hormann & Zimmer, 2016).

Since emulsions have been widely used as novel carriers for functional nutrients, a better understanding of the factors that can influence the digestion behavior of emulsion droplets and thus the release of encapsulated bioactive nutrients becomes very important. The digestion of emulsion droplets is closely related to their structure, including the oil phase, interfacial layer, and water phase. Taking protein stabilized oil-in-water (O/W) emulsion as an example, the digestion process of protein-stabilized emulsion droplets containing bioactive nutrients mainly goes through four steps: (i) binding of proteinase to the droplet surface in the water phase, e.g., pepsin and trypsin; (ii) hydrolysis of interfacial protein layers by proteinase; (iii) hydrolysis of lipid in the oil phase by lipase and release of bioactive nutrients from lipid droplets; and (iv) formation of bile-salt emulsified micelles containing released lipophilic bioactive nutrients. Accordingly, the formula of water phase and interface can influence the final bioaccessibility by modifying the first two steps of the digestion, while the structure and composition of oil phase can influence the final bioaccessibility through affecting the later two steps of digestion. The effects of composition or structure of the oil phase and interface

on the release of encapsulated bioactive nutrients from emulsions have been well investigated in previous studies (Lu et al., 2017b; Qian, Decker, Xiao, & McClements, 2012; Salvia-Trujillo, Fumiaki, Park, & McClements, 2017). However, little is known about the influence of the water phase on the digestion of emulsion droplets and thus the release of encapsulated nutrients from emulsions.

Natural polysaccharides are a class of biopolymers that have been widely used in the production of emulsions, due to their wide availability, good physical and chemical stability, edibility, and low cost. Previous studies have shown that introducing polysaccharide as a second stabilizer into the water phase can significantly enhance the stability of emulsions (Dickinson, 2011). Polysaccharides can generally modify the interface, rheology, or gelation properties of emulsions. Polysaccharides can also significantly enhance the stability of protein-stabilized emulsions by forming a polysaccharide-protein double-layer interface (Aoki, Decker, & McClements, 2005; Guzey, Kim, & McClements, 2004; Jeonghee Surh 2005; Mao, Roos, & Miao, 2015). In addition, polysaccharides can form network structures in the water phase, which can limit the mobility of oil droplets by steric hindrance and thus improve the creaming stability of emulsions (Lin et al., 2017). Such network structures in the water phase can potentially also influence the binding and interaction process of enzymes, the digestion velocity of emulsion droplets, and thus the release of encapsulated bioactive nutrients, as described above.

Konjac glucomannan (KGM) is a natural polysaccharide obtained from tubers of *Amorphophallus konjac* cultivated in Asia. KGM is reported to possess many health benefits, such as lowering the blood cholesterol and sugar levels, positively modulating gut microflora, promoting weight loss, and improving immune function (Arvill, 1995; Chua, Baldwin, Hocking, & Chan, 2010). However, there are few studies on using KGM to modify the water phase and thus influencing the release of encapsulated bioactive nutrients from emulsions.

Introducing KGM into emulsions can also endow the final emulsions with new health benefits associated with KGM besides those contributed by encapsulated molecules. This can accordingly achieve a delivery of multiple nutrients in one carrier.

From the above, this study was therefore proposed to investigate the effect of structuring water phase of model oil-in-water (O/W) emulsions by KGM on their properties, including droplet size, surface charge, creaming stability, pH stability, thermal stability, and freeze-thaw stability, and also the effect on the release of encapsulated bioactive nutrients (β-carotene) from O/W emulsion after passing through a simulated gastrointestinal tract (GIT) digestion.

2. Material and methods

2.1 Materials

Konjac glucomannan powder was obtained from Konjac Food (Cupertino, CA, USA). Whey protein isolate was purchased from Davisco Food International (Le Sueur, MN, USA). β-carotene (>93%, UV), pepsin, pancreatin (porcine, 4×USP) were purchased from Sigma-Aldrich (St. Louis, MO, USA). Sunflower oil was purchased from a local supermarket. All other chemicals and reagents used were of AR-grade and obtained from Sigma-Aldrich (St. Louis, MO, USA).

2.2 Preparation of emulsions

Whey protein isolate (WPI) was dispersed (2%, w/w) in Millipore water containing sodium azide as antimicrobial agent (0.01% w/w). The dispersions were stirred for 4 h and kept at 4 °C overnight for complete dissolution of WPI. The dispersion was then brought to 25 °C before adding konjac glucomannan (KGM) powder to make a KGM content of 0.05%, 0.1%, or 0.2% in the final emulsions. The mixtures were stirred for 4 h for a complete dissolution of

KGM and then centrifuged at 4,000 rpm (2700 g) for 20 min before being used as the water phase. The oil phase was prepared by dissolving β-carotene (0.2%, w/w in final emulsion) in sunflower oil (10%, w/w in final emulsion) at 140 °C which was then mixed with the water phase at 10,000 rpm for 2 min at room temperature using an Ultra-Turrax (IKA, Staufen, Germany) followed by further homogenization (APV 1000, SPX Flow Technology, Charlotte, North Carolina, USA) at 50 MPa for 3 passes at room temperature to obtain final emulsions.

2.3 Droplet size and surface charge

The droplet size and zeta potential of KGM emulsions were measured by a laser particle analyzer (Nano-ZS, Malvern Instruments, Worcestershire, UK) as described in our previous study (Lu et al., 2016). Emulsions were diluted to the final oil content (w/w) of 0.01% before testing. The refractive index (RI) of samples was set at 1.47 for sunflower oil.

2.4 Creaming stability

Emulsion stability was evaluated using Lumisizer (LUM GmbH, Berlin, Germany) as describe previously. Emulsions were centrifuged at 2,300 g at 25 °C with a scanning rate of once every 10 s for 1,200 s. Following the test, curves of the integrated transmitted light against time were plotted, and the slope of each curve was taken as the Creaming Index (CI).

2.5 Rheological analysis

Rheological measurements were performed using an AR 2000ex rheometer (TA Instruments, Crawley, UK). A concentric cylinder geometry (stator inner radius=15 mm, rotor outer radius=14 mm) was selected, and 19 g of each sample was placed into the inner cylinder and equilibrated for 2 min before measurement. Viscosity testing was performed over a shear rate range of 0–300 s^{-1} at 25 °C.

98

99 *2.6 Fourier transforms infrared spectroscopy (FT-IR)*

100 Fourier transform infrared spectroscopy (FT-IR) technology was used to evaluate the
101 molecular structure of KGM and WPI in water phase before and after homogenization. The
102 IR spectra of the samples were recorded by FT-IR spectrophotometer (Bruker Corp, Billerica,
103 Massachusetts, USA) using an attenuated total reflection (ATR) technique. The spectrum was
104 scanned from 4000 cm^{-1}-900 cm^{-1} with a resolution of 4 cm^{-1}. An average of 300 scans was
105 recorded for each sample.

106

107 *2.7 Stability of emulsions at different pH values and temperature*

108 The effect of KGM on the resistance of emulsions to extreme pH environments was
109 evaluated. The KGM emulsions were brought to different pH values from 2.0 to 7.0 with HCI
110 or NaOH solution, and maintained for 4 h at room temperature before droplet size, surface
111 charge and creaming stability analysis by DLS and Lumisizer as described above.

112 The effect of KGM on the resistance of emulsions to thermal processing was evaluated
113 following incubation at 25°C, 37 °C, or 80 °C for 2 h. The droplet size was then analyzed by
114 Malvern Nanosizer as described above.

115

116 *2.8 Freeze-Thaw Test*

117 Freeze-thaw testing was applied to emulsions with the objective of assessing the possibility
118 of frozen storage of liquid emulsions containing bioactive nutrients. In addition, the changes
119 in properties of emulsions after the freeze-thaw processing can potentially contribute to the
120 freeze-drying of liquid emulsions into solid products, which can significantly facilitate the
121 storage, transportation, and application of emulsions.

Liquid emulsions were kept at -20°C for 24 h and then thawed at 25°C for 2 h in a water bath. This cycle was repeated three times. Droplet size and surface charge was measured after each cycle by Malvern nanosizer. Creaming stability of emulsions after three cycles was measured with Lumisizer as described above.

Oiling-off of emulsions after 3 cycles of freeze-thaw was also evaluated by measuring the content of β-carotene in the free oil fraction. The thawed emulsions were centrifuged at 10,000 g for 10 min (25 °C). Free oil layer containing β-carotene on top of emulsions were collected and subjected to a second centrifuge at 4000 g for 10 min (25 °C). The supernatant (free oil) containing β-carotene was collected and extracted with ethanol/hexane. The content of β-carotene in hexane fraction was quantified by RP-HPLC as described below. The oiling-off was calculated based on the equation below:

$$\text{Oil-off (\%)} = \frac{C_{\text{free oil}}}{C_{\text{initial}}} \times 100\% \qquad (1)$$

where $C_{\text{free oil}}$ and C_{initial} are the concentration of β-carotene in the free oil fraction after 3 cycles of freeze-thaw and in the initial emulsion before freeze-thaw test, respectively.

2.9 Simulated gastrointestinal tract (GIT) digestion

An *in vitro* simulated GIT model consisting of mouth, gastric and intestinal phases was used to digest β-carotene loaded emulsions. The simulated saliva fluid (SSF), simulated gastric fluid (SGF), and simulated intestinal fluid (SIF) were prepared as described previously research (Lu et al., 2017b) with minor modification.

For the mouth phase digestion, emulsions were mixed with SSF (1:1, v/v), the pH was adjusted to 6.8 and the mixtures were incubated at 37 °C for 10 min with continuous agitation at 150 rpm.For the gastric phase, the bolus sample from the mouth phase was mixed with the SGF (1:1, v/v). The pH of the mixture was adjusted to 2.5 and it was incubated at 37 °C for 2

h with continuous agitation at 150 rpm. The pepsin activity in the final mixture was 1000 U/ml. For the small intestinal phase, the bolus sample from the gastric phase was mixed with the SIF (1:1, v/v). The pH of the mixture was adjusted to 7.0 and it was incubated at 37 °C for 2 h with continuous agitation at 150 rpm. The trypsin activity in the final mixture was 25 U/ml.

2.10 Laser scanning confocal microscope observation

The microstructure of the initial and digested samples was observed using a Leica TCS SP5 laser scanning confocal microscope (Leica Microsystems, Baden-Württemberg, Germany). All the images were taken using a 63 x oil-immersion objective and simultaneous dual-channel imaging, He-Ne laser (excitation wavelength at 633 nm) and an Argon laser (excitation wavelength at 488 nm). A mixture of two dyes, Fast green (0.1 %, w/w in water) and Nile red (0.1 %, w/w in propanediol) was used to color and detect protein and lipid, respectively. Initial/digested sample (500 µl) was gently mixed with 50 µl of mixed dye.

2.11 Release of encapsulated β-carotene

The amount of β-carotene in micelle fractions after the intestinal phase GIT was measured as the final release rate of encapsulated β-carotene. Briefly, an aliquot of raw digesta from the intestinal phase was centrifuged at 4,500 rpm (2978 g) for 40 min at 4 °C and the middle layer was collected and considered as the micelle fraction. One mL of the micelle fraction was extracted twice with ethanol/n-hexane. The upper n-hexane layer containing the solubilized β-carotene was collected and analyzed by RP-HPLC as described below.

The final release rate of encapsulated β-carotene was calculated using the follow equation:

$$\text{Release rate (\%)} = \frac{C_{\text{micelle}}}{C_{\text{initial}}} \times 100\% \qquad (2)$$

where $C_{micelle}$ and $C_{initial}$ are the concentration of β-carotene in the micelle fraction and initial emulsion before digestion, respectively.

2.12 Quantification of β-carotene

Reversed-phase high performance liquid chromatography (RP-HPLC) was used to quantify β-carotene. An Agilent 1200 series system with a DAD UV-Vis detector (Agilent, Santa Clara, CA, USA) and a reversed phase TSKgel ODS-100v C_{18} column (4.6×250 mm, 5 μm, TOSOH) was employed.

Chromatography conditions: column operation temperature at 30 °C; elution was performed with 90% ethanol and 10% acetonitrile from 0-30 min, flow rate was 1 mL/min, detection wavelength was 450 nm, and injection volume was 20 μL.

2.13 Statistical analysis

All experiments were repeated at least three times. One-way analysis of variance (ANOVA) was employed to compare means of data. A t-Test was used to determine the differences between means. Significant differences were determined at the 0.05 level ($p<0.05$).

3. Results and discussion

3.1 Droplet size and surface charge

As is shown in Table 1, an emulsion without konjac glucomannan (KGM) had an average droplet size of 252 nm, while emulsions containing KGM showed significantly increased droplet size with increasing KGM content from 0.05% to 0.2% ($p<0.05$). KGM, as a natural polysaccharide, is dispersible in water and can form a network structure with different

particle size depending on its molecular weight and concentration (Lazaridou, Biliaderis, & Izydorczyk, 2003). This network structure can potentially increase the average droplet size of emulsions. However, the droplet size test was performed after 1000-fold dilution of emulsions and KGM at this extreme low concentration (<0.0002%) is unlikely to form a network structure.

There is another possibility to explain the increased droplet size of KGM-emulsions. The peak of the size distribution shifted to a slightly higher value (data not shown), indicating that there may be some flocculation or coalescence of the droplets, which were forced close enough at high KGM concentrations induced by depletion attraction between droplets (Ye, Hemar, & Singh, 2004). Slight aggregation of droplets was also observed in our previous research (Lu et al., 2016).

All emulsions were negatively charged and no significant difference in surface charge between different emulsions was observed (p>0.05). Generally, KGM is a non-charged polysaccharide and binding of KGM to the surface of WPI-stabilized emulsion droplets should lead to their significantly reduced surface charge. However, surface charge of emulsions containing KGM showed almost no difference from that of the emulsion without KGM (Table 1), potentially demonstrating that there is very limited binding of KGM to the droplet surface.

3.2 Rheological analysis

The viscosity of emulsions significantly decreased with the increasing shear rate (~50 1/s), indicating a shear-thinning property. The KGM emulsion showed higher viscosity than emulsion without KGM, and the viscosity of KGM emulsions increased with increasing KGM content (Fig. 1). Several factors can potentially influence the viscosity of emulsions, such as oil content, viscosity of water phase, droplet size, or surface charge (McClements,

2015). In this study, increased viscosity of KGM emulsions can be mainly attributed to two factors: (i) increased viscosity of water phase (WPI-KGM dispersion); and (ii) flocculation of droplets by depletion force induced by non-absorbed polysaccharide KGM. As shown in Fig. 2, the viscosity of the water phase (WPI-KGM dispersions) also decreased with increasing shear rate, and a similar increase in viscosity with increasing KGM content was seen, suggesting that KGM can significantly increase the viscosity of the water phase and thus the viscosity of final emulsions. In addition, KGM, as a biopolymer can potentially generate a depletion force between droplets and induce flocculation of droplets at certain concentrations (Mao, 1995), which accordingly can increase the viscosity of emulsions. This point will be further discussed in the creaming stability section below.

Generally, KGM can disperse in water and form highly viscous suspensions at pH values of 4.0-7.0 due to its high molecular weight, ranging from 200-2000 kDa (Chua et al., 2010; Villay et al., 2012). The viscosity of WPI-KGM suspensions after homogenization decreased significantly (**Fig. 2**). This is mainly attributed to the mechanical de-polymerization and/or de-polymerization-coupled conformation of KGM by homogenization (Villay et al., 2012). The molar-mass distribution is the primary parameter that influences the viscosity of polysaccharide in solution. Homogenization can lead to mechanical degradation (de-polymerization) of polysaccharides, and produce fractions with low molecular weight or low polydispersity, which accordingly lead to decreased viscosity.

3.3 Fourier- transform infrared spectroscopy (FT-IR) analysis

Generally, polysaccharides can form double layer structures at the interface of protein-stabilized emulsion through electrostatic attraction, hydrogen bond or hydrophobic interactions with protein. However, KGM is a non-charged polysaccharide and cannot form complexes with protein by electrostatic attraction. Our preliminary research also indicated

that there is no significant hydrophobic or hydrogen bond interaction between WPI and KGM at different pH values (2-8) and temperatures (up to 90℃) (data not shown).

However, little was known about the interaction between WPI and KGM in the water phase after homogenization. Hence, fourier-transform infrared spectroscopy (FT-IR) was employed to investigate the influence of HPH on the properties of water phase. The spectra of water phase (WPI-KGM dispersions) before and after HPH were collected within wavelengths of 900-4000 cm^{-1} and spectra between 1350-1700 cm^{-1} were analysed, since this zone covers the main characteristic absorption peaks of WPI (Chen, Li, Ding, & Suo, 2012). The spectra of WPI (Fig. 3) indicated the presence of characteristic absorption peaks at 1645, 1548, 1456, and 1400 cm^{-1} corresponding to the C=O stretching and the bending of N-H, C-H, C-N bonds, respectively (Barth, 2007; Chen et al., 2012). Compared with WPI before homogenization, the spectra of WPI after homogenization did not show significant difference.

KGM exhibited a characteristic absorption peak of the β-1,4-linked glycosidic bond at 895 cm^{-1} and a characteristic peak of the enlargement of pyranoid rings at 808 cm^{-1} (Gao, Su, Huang, & He, 2014). Hence, KGM showed almost no significant absorption within wavelength of 900-4000cm^{-1}. Spectra of WPI-KGM dispersions also showed no significant difference compared with pure WPI dispersion before and after homogenization (Fig. 3). All these results suggested that: (i) homogenization did not induce significant changes in the molecular structure of WPI; and (ii) homogenization processing did not induce obvious non-covalent interactions, e.g., electrostatic attraction, hydrophobic interaction or hydrogen bond, between WPI and KGM. However, the droplet size (data not shown) of WPI-KGM dispersions significantly decreased after homogenization, which was mainly attributed to the mechanical de-polymerization of KGM by homogenization, as described above (Villay et al., 2012).

3.4 Creaming stability

Creaming index (CI) was used to describe the rate of light transmission change. It is calculated based on the curve of the integrated transmitted light against time. A higher CI value indicates a lower creaming stability of emulsion. Hence, emulsion containing 0.05% KGM showed the highest creaming stability, followed by emulsions containing 0.1% KGM and the emulsion without KGM (Table 1). KGM can improve the creaming stability of emulsions by increasing the viscosity of emulsions as described above (Fig. 1). In addition, KGM at these concentrations (0.05%, or 0.1%) can potentially form a network structure in water phase. Even though, these network structures can be destroyed by mechanical homogenization as described above, the chain-structure of KGM can still limit the creaming of emulsions due to the increased steric hindrance and force of friction between droplets and the continuous phase.

However, emulsion containing 0.2% KGM showed very poor creaming stability, which was mainly attributed to the depletion flocculation of emulsion droplets by non-absorbed KGM (Klinkesorn, Sophanodora, Chinachoti, & McClements, 2004; Mao, 1995). Non-adsorbed polymers can generate an attractive osmotic force between droplets. This osmotic force increases with increasing concentration of polymer until it is large enough to overcome the repulsive forces between droplets and cause flocculation of droplets. Droplet flocculation can also increase the viscosity of emulsions by decreasing the internal packing of droplets within flocs due to increased effective volume fraction of the particles based on Dougherty-Krieger equation (McClements, 2015). This may explain why emulsion with high content of KGM showed increased viscosity, as described above (Fig. 1).

3.5 Stability of emulsions at different pH

Emulsions were all stable at pH 2-4 and pH 6-7. The emulsion without KGM showed a significantly increase in droplet size at pH 5 (Fig. 4a), which is mainly attribute to whey protein aggregation at this pH value, which is close to its isoelectric point (IEP). This increase in droplet size accordingly resulted in poor creaming stability of these emulsions (Table 2). Emulsions containing KGM showed significantly less increase in droplet size at pH 5 (p<0.05) than the emulsion without KGM, depending on the content of KGM. Accordingly, these KGM-containing emulsions with reduced droplet size at pH 5 showed better creaming stability than the emulsion without KGM (Table 2). These results suggested that KGM can significantly improve the pH stability of WPI-stabilized emulsions.

KGM is a very stable polysaccharide across a wide range of pH values. KGM, with a chain-like structure, can fill in the space between free protein molecules and oil droplets in emulsions and potentially can isolate oil droplets from each other, which accordingly reduces the Brownian-motion-induced contact of proteins and oil droplets and thus their aggregation at pH value close to the IEP of proteins. The higher of the KGM content, the higher density of the filled space, and thus the more significant inhibition of aggregation.

3.6 Thermal stability

The thermal stability of emulsions at different temperatures was also investigated. After 2 h incubation at elevated temperature (37℃ or 80℃), the droplet size of all emulsions showed almost no difference compared to the droplet size of emulsions at 25℃ (Table 2), suggesting that emulsions in this study had good thermal stability at temperatures up to 80℃.

3.7 Freeze-thaw testing

After the first cycle of freeze-thaw, the droplet size and surface charge of all emulsions significantly decreased (p<0.05) (Table 3). Then, the droplet size increased with the

318 increasing freeze-thaw cycles and the final droplet size of all emulsions after three cycles
319 were smaller than their initial droplet size. No significant difference in surface charge after
320 second and third cycles of freeze-thaw was observed, except for the emulsion without KGM.
321 Oiling-off of emulsions was also clearly observed after 3 cycles of freeze-thaw (Table 2) and
322 KGM successfully reduced the oiling-off of the emulsion. Compared with the emulsion
323 without KGM (10.2%), only 2.4% of the oil was released from the emulsion containing 0.2%
324 KGM after 3 cycles of freeze-thaw ($p<0.05$).

325 Ice crystals are formed during freezing of emulsions, and the ice penetration can
326 potentially lead to the break-down of the protein layer surrounding the oil droplets, and thus
327 lead to oiling-off of emulsions. Combined with the results above, it is assumed that (i)
328 freezing led to the break-down of large emulsion droplets, leading to the oiling-off of
329 emulsions, a narrower size distribution and a smaller average droplet size, and (ii) freezing
330 can also induce desorption of whey proteins from the droplet surface, leading to the reduced
331 surface charge of emulsions after first cycle of freeze-thaw. However, the above findings
332 suggested that KGM can help to maintain the structure of the interfacial protein layer and
333 significantly protect the emulsion from oiling-off, probably by slowing down the formation
334 of ice crystals (Mao et al., 2015).

335

336 *3.8 Simulated GIT digestion*

337 As described in our previous studies (Lu, Kelly, & Miao, 2017a; Lu et al., 2017b), passing
338 emulsions through simulated gastrointestinal tract (GIT) digestion greatly modifies their
339 properties. The average droplet size of all emulsions significantly increased after gastric
340 phase and decreased after intestinal phase (Table 4), which was also confirmed by the
341 microscopy observation. As is shown in Fig. 5, after the mouth phase, no major difference in
342 droplet shape and size was observed. After the gastric phase, significant aggregation of

proteins (green fluorescence) was observed, which was mainly attributed to the exposure of the hydrophobic domain of whey proteins induced by pepsin hydrolysis and relatively high ionic strength in gastric phase. The process of protein aggregation also clustered some oil droplets (red fluorescence) and formed larger complexes. In addition, hydrolysis of WPI at the interface by pepsin resulted in aggregation of some oil droplets. These two factors may explain the dramatic increase in droplet size after the gastric phase. After the intestinal phase, almost all proteins at the interface were hydrolysed by trypsin, leading to the collapse of oil droplets and the hydrolysis of oil by lipase. The hydrolysis of whey protein and sunflower oil also led to the quenching of most of the green and red fluorescence, respectively. Only very few intact oil droplets were captured.

3.9 Release of encapsulated β-carotene after GIT

Adding KGM to the water phase of emulsions significantly modified the release of β-carotene from emulsion droplets after passing through GIT. Emulsion without KGM showed a final β-carotene-release-rate of 64.5%. β-carotene-release-rate of emulsions containing KGM were generally inferior to that of emulsion without KGM, and the release rate decreased with increasing KGM content (**Fig. 6**). Emulsions containing 0.1% KGM and 0.2% KGM showed significant lower β-carotene-release-rate than emulsion without KGM ($p<0.05$). The results indicated that KGM can potentially slow down the release of β-carotene from emulsion droplets, which is dependent on the content of KGM in final emulsions.

As discussed in the introduction section, any factors that influence the four steps of the digestion process of emulsion droplets can potentially modify the final release of encapsulated ingredients from emulsions. Our previous studies also showed that emulsions with maltodextrin-structured water phase showed significantly different release profiles of lipophilic food flavors due to modified mobility within the water phase (Mao, Roos, & Miao,

2014). In this study, KGM was used to formulate the water phase of model O/W emulsion. Emulsions with KGM showed more a viscous water phase than emulsion without KGM. In addition, KGM shows a chain-like molecular structure in water, which facilitates intermolecular cross-linking into a gel-like structure. All these properties can potentially interfere with the digestion steps of the hydrolysis of interfacial protein layer and the hydrolysis of oil phase by steric hindrance effect, leading to slower release of encapsulated ingredients from emulsion droplets. These factors may explain why emulsions with KGM-structured water phase showed decreased release rates of encapsulated β-carotene with increasing KGM content in this study. The findings also suggest that it is feasible to achieve a controlled/sustainable release of encapsulated functional ingredients from emulsions by structuring the water phase of emulsions with natural biopolymers.

However, KGM can be hydrolysed and utilized by the microorganisms in the gut. Hence, the *in-vivo* digestion behaviour and release profile of encapsulated ingredients in emulsions with a KGM-structured water phase need to be further studied.

4. Conclusion

Konjac glucomannan (KGM) increased the viscosity of the water phase and thus the viscosity of the final whey-protein-isolate (WPI) stabilized O/W emulsions. No significant non-covalent interaction between KGM and whey proteins before and after homogenization was observed by FT-IR. KGM greatly improved the creaming and pH stability of emulsions and protected emulsions from oiling-off after freeze-thaw process. The digestion and break-down of emulsion droplets mainly happened in the intestinal phase of a simulated gastrointestinal tract (GIT), as evaluated by confocal laser scanning microscopy. KGM significantly decreased the release rate ofβ-carotene from emulsions, which is dependent on the content of KGM in emulsions.

Model O/W emulsions with better stability and controlled release of β-carotene were obtained by simply structuring the water phase with a health-beneficial polysaccharide, KGM. Findings in this study make it possible to design emulsion-based functional food products or drug carriers with potential controlled or sustainable release of functional ingredients inside by structuring the water phase of emulsions with natural edible biopolymers.

Acknowledgement

The assistance of Ana Isabel Mulet Cabero with the laser scanning confocal microscope observation was highly acknowledged.

Funding

This work was supported by National Natural Science Foundation of China (No.31628016), China Scholarship Council (No.201508300001), and Teagasc-The Irish Agriculture and Food Development Authority (RMIS6821)

Notes

The authors declare no conflict of interest.

References

Aoki, T., Decker, E. A., & McClements, D. J. (2005). Influence of environmental stresses on stability of O/W emulsions containing droplets stabilized by multilayered membranes produced by a layer-by-layer electrostatic deposition technique. *Food Hydrocolloids, 19*(2), 209-220.

Arvill, A. B., Lennart. (1995). Effect of short-term ingestion of konjac glucomannan on serum cholesterol in healthy men. *Am J Clin Nutr, 61*, 585-589.

Barth, A. (2007). Infrared spectroscopy of proteins. *Biochim Biophys Acta, 1767*(9), 1073-1101.

Chen, B., Li, H., Ding, Y., & Suo, H. (2012). Formation and microstructural characterization of whey protein isolate/beet pectin coacervations by laccase catalyzed cross-linking. *LWT - Food Science and Technology, 47*(1), 31-38.

Chua, M., Baldwin, T. C., Hocking, T. J., & Chan, K. (2010). Traditional uses and potential health benefits of Amorphophallus konjac K. Koch ex N.E.Br. *Journal of Ethnopharmacology, 128*(2), 268-278.

Dickinson, E. (2011). Mixed biopolymers at interfaces: Competitive adsorption and multilayer structures. *Food Hydrocolloids, 25*(8), 1966-1983.

Guzey, D., Kim, H. J., & McClements, D. J. (2004). Factors influencing the production of o/w emulsions stabilized by β-lactoglobulin–pectin membranes. *Food Hydrocolloids, 18*(6), 967-975.

Hormann, K., & Zimmer, A. (2016). Drug delivery and drug targeting with parenteral lipid nanoemulsions - A review. *Journal of Controlled Release, 223*, 85-98.

Jeonghee Surh , Y. S. G., Eric A. Decker , and D. Julian McClements. (2005). Influence of Environmental Stresses on Stability of Emulsions Containing Cationic Droplets Stabilized by SDS Fish Gelatin Membranes. *J. Agric. Food Chem., 53*, 4236-4244.

Karthik, P., & Anandharamakrishnan, C. (2016). Enhancing omega-3 fatty acids nanoemulsion stability and in-vitro digestibility through emulsifiers. *Journal of Food Engineering, 187*, 92-105.

Klinkesorn, U., Sophanodora, P., Chinachoti, P., & McClements, D. J. (2004). Stability and rheology of corn oil-in-water emulsions containing maltodextrin. *Food Research International, 37*(9), 851-859.

Lazaridou, A., Biliaderis, C. G., & Izydorczyk, M. S. (2003). Molecular size effects on rheological properties of oat β-glucans in solution and gels. *Food Hydrocolloids, 17*(5), 693-712.

Lin, D., Lu, W., Kelly, A. L., Zhang, L., Zheng, B., & Miao, S. (2017). Interactions of vegetable proteins with other polymers: Structure-function relationships and applications in the food industry. *Trends in Food Science & Technology, 68*, 130-144.

Lu, W., Kelly, A. L., Maguire, P., Zhang, H., Stanton, C., & Miao, S. (2016). Correlation of Emulsion Structure with Cellular Uptake Behavior of Encapsulated Bioactive Nutrients: Influence of Droplet Size and Interfacial Structure. *J Agric Food Chem, 64*, 8659-8666.

Lu, W., Kelly, A. L., & Miao, S. (2016). Emulsion-based encapsulation and delivery systems for polyphenols. *Trends in Food Science & Technology, 47*, 1-9.

Lu, W., Kelly, A. L., & Miao, S. (2017a). Bioaccessibility and Cellular Uptake of beta-Carotene Encapsulated in Model O/W Emulsions: Influence of Initial Droplet Size and Emulsifiers. *Nanomaterials (Basel), 7*(9), 282-292.

Lu, W., Kelly, A. L., & Miao, S. (2017b). Improved Bioavailability of Encapsulated Bioactive Nutrients Delivered through Monoglyceride-Structured O/W Emulsions. *Journal of Agricultural and Food Chemistry, 65*, 3048-3055.

Mao, L., Roos, Y. H., & Miao, S. (2014). Study on the rheological properties and volatile release of cold-set emulsion-filled protein gels. *J Agric Food Chem, 62*(47), 11420-11428.

Mao, L., Roos, Y. H., & Miao, S. (2015). Effect of maltodextrins on the stability and release of volatile compounds of oil-in-water emulsions subjected to freeze–thaw treatment. *Food Hydrocolloids, 50*, 219-227.

McClements, D. J. (2015). *Food emulsions: principles, practices, and techniques* (Third ed.). New York: CRC press.

Niu, Z., Conejos-Sanchez, I., Griffin, B. T., O'Driscoll, C. M., & Alonso, M. J. (2016). Lipid-based nanocarriers for oral peptide delivery. *Adv Drug Deliv Rev, 106*(Pt B), 337-354.

Qian, C., Decker, E. A., Xiao, H., & McClements, D. J. (2012). Nanoemulsion delivery systems: influence of carrier oil on beta-carotene bioaccessibility. *Food Chem, 135*(3), 1440-1447.

Salvia-Trujillo, L., Fumiaki, B., Park, Y., & McClements, D. J. (2017). The influence of lipid droplet size on the oral bioavailability of vitamin D2 encapsulated in emulsions: an in vitro and in vivo study. *Food Funct, 8*, 767-777.

Villay, A., Lakkis de Filippis, F., Picton, L., Le Cerf, D., Vial, C., & Michaud, P. (2012). Comparison of polysaccharide degradations by dynamic high-pressure homogenization. *Food Hydrocolloids, 27*(2), 278-286.

Y. Mao, M. E. C., H.N.W. Lekkerkerker. (1995). Depletion force in colloidal systems. *Physica A, 222*, 10-24.

Ye, A., Hemar, Y., & Singh, H. (2004). Enhancement of coalescence by xanthan addition to oil-in-water emulsions formed with extensively hydrolysed whey proteins. *Food Hydrocolloids, 18*(5), 737-746.

Zhao Gao, Rongxin Su, Renliang Huang, and, W. Q., & He, Z. (2014). Glucomannan-mediated facile synthesis of gold nanoparticles for catalytic reduction of 4-nitrophenol. *Nanoscale Research Letters, 9*, 8.

Figure captions

Fig. 1 Viscosity of emulsions. KGM 0% indicates emulsion without konjac glucomannan (KGM), while KGM 0.05%, KGM 0.1%, and KGM 0.2% indicates emulsions with KGM content (w/w) of 0.05%, 0.1%, and 0.2%, respectively. Insert: initial viscosity at very low shear rate (~2.5 1/s)

Fig. 2 Viscosity of whey protein isolate (WPI) and konjac glucomannan (KGM) mixed solutions before and after homogenization at 50 MPa. (**a**) WPI solution without KGM; (**b**) WPI solution with 0.05% (w/w) KGM; (**c**) WPI solution with 0.1% KGM; (**d**) WPI solution with 0.2% KGM.

Fig. 3 Fourier-transform infrared (FT-IR) spectra of (a) WPI (2%, w/w), (b) WPI (2%, w/w) after homogenization , (c) a mixture of WPI (2%, w/w) and KGM (0.2%, w/w) and (d) a mixture of WPI (2%, w/w) and KGM (0.2%, w/w) after homogenization. WPI indicates whey protein isolate. KGM indicates konjac glucomannan.

Fig. 4 Droplet size (**a**) and zeta potential (**b**) of emulsions at different pH values. KGM 0% indicate emulsion without konjac glucomannan (KGM). KGM 0.05%, KGM 0.1%, and KGM 0.2% indicates emulsions with KGM content of 0.05%, 0.1%, and 0.2%, respectively.

Fig. 5 Confocal scanning microscope observation of emulsion droplets after being exposed to simulated gastrointestinal tract (GIT). KGM 0% indicate emulsion without konjac glucomannan (KGM). KGM 0.05%, KGM 0.1%, and KGM 0.2% indicates emulsions with KGM content (w/w) of 0.05%, 0.1%, and 0.2%, respectively.

Fig. 6 Release of encapsulated β-carotene from emulsions. KGM indicates konjac glucomannan. * $p<0.05$, ** $p<0.01$.

Table 1 Droplet size, zeta potential, polydispersity index (PdI) and creaming index (CI) of emulsions containing KGM

KGM (%, w/w)	size (d.nm)	zeta potential (mV)	PdI	CI (%/min)
0	252±9[d]	-65.0±5.4[a]	0.24±0.02[a]	0.64±0.01[b]
0.05	280±8[c]	-60.4±2.2[a]	0.21±0.02[b]	0.52±0.02[c]
0.1	306±17[b]	-59.3±2.6[a]	0.21±0.01[b]	0.55±0.02[c]
0.2	350±24[a]	-59.3±0.7[a]	0.20±0.02[b]	1.70±0.04[a]

*KGM indicates konjac glucomannan. [a]Different letters indicate significant difference between values in a column (p<0.05)

Table 2 Creaming index (CI) of emulsions at pH 5.0 or after freeze-thaw, oil-off of emulsions after freeze-thaw, and droplet size of emulsions at different temperatures

KGM content (%, w/w)	CI at pH 5.0 (%/min)	CI after freeze-thaw (%/min)	Oil-off after freeze-thaw (%)	Size (d.nm)		
				25 °C	37 °C	80 °C
0	9.11±0.05[a]	0.76±0.00[b]	10.2±0.03[a]	252±8[d]	254±5[d]	257±2[d]
0.05	7.77±0.03[b]	0.70±0.00[c]	6.7±0.02[b]	271±10[c]	269±9[c]	266±6[c]
0.1	5.98±0.03[c]	0.62±0.00[d]	4.8±0.00[c]	313±6[b]	312±6[b]	314±6[b]
0.2	3.88±0.04[d]	1.36±0.01[a]	2.4±0.02[d]	334±6[a]	328±6[a]	331±6[a]

*KGM indicates konjac glucomannan. [a]Different letters indicate significant difference between values in a column (p<0.05)

Table 3 Droplet size and surface charge of emulsions after freeze-thaw processing

Freeze-thaw cycle	Size (d.nm)				Zeta potential (mV)			
	KGM 0%	KGM 0.05%	KGM 0.1%	KGM 0.2%	KGM 0%	KGM 0.05%	KGM 0.1%	KGM 0.2%
0	252±9^{a}	280±8^{a}	306±17^{a}	350±24^{a}	-65.0±5.4^{a}	-60.4±2.2^{a}	-59.3±2.6^{a}	-59.3±0.7^{a}
1	202±4^{b}	226±2^{b}	266±18^{b}	302±18^{b}	-57.3±0.1^{b}	-52.6±1.4^{b}	-53.1±2.1^{b}	-52.8±0.7^{b}
2	216±5^{c}	249±8^{c}	288±16^{c}	308±13^{b}	-52.5±1.8^{c}	-54.5±1.8^{b}	-53.9±1.8^{b}	-52.4±1.3^{b}
3	227±6^{d}	273±9^{d}	307±9^{d}	314±10^{b}	-52.5±1.7^{c}	-54.2±1.4^{b}	-51.4±0.1^{b}	-54.5±0^{b}

* Freeze-thaw test was done at -20°C, followed by thawing at 25°C. KGM 0% indicate emulsion without konjac glucomannan (KGM). KGM 0.05%, KGM 0.1%, and KGM 0.2% indicates emulsions with KGM content (w/w) of 0.05%, 0.1%, and 0.2%, respectively. ^{a}Different letters indicate significant difference between values in a column (p<0.05)

Table 4 Droplet size and zeta potential of emulsions containing KGM following different phases of gastrointestinal tract digestion

KGM content (w/w, %)	Size (d.nm)				zeta potential (mV)			
	initial	mouth phase	gastric phase	intestinal phase	initial	mouth phase	gastric phase	intestinal phase
0	252±9[d]	248±1[d]	1505±361[a]	192±56[a]	-65±5.4[a]	-64.5±4.9[a]	18.0±1.4[a]	-70.5±6.4[a]
0.05	280±8[c]	288±1[c]	1624±452[a]	185±31[a]	-60.4±2.2[a]	-58.5±0.7[a]	15.5±0.7[a,b]	-71.0±2.8[a]
0.1	306±17[b]	305±4[b]	1598±423[a]	178±19[a]	-59.3±2.6[a]	-59.5±2.1[a]	14.0±0[b]	-76.5±4.9[a]
0.2	350±24[a]	352±11[a]	1057±204[a]	200±38[a]	-59.3±0.7[a]	-59.0±1.4[a]	9.0±0[c]	-77.5±3.5[a]

*KGM indicates konjac glucomannan. [a]Different letters indicate significant difference between values in a column (p<0.05)

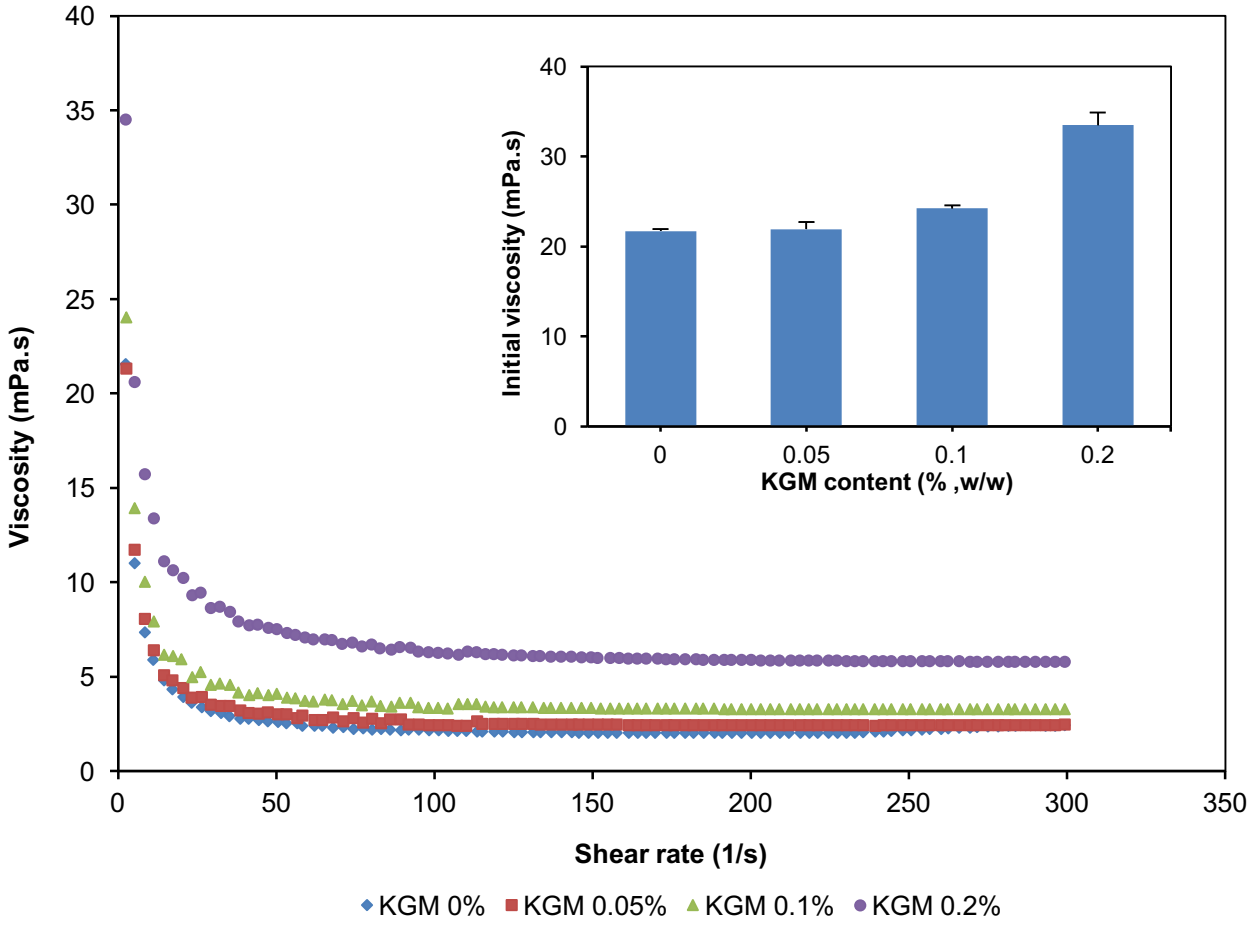

Fig. 1

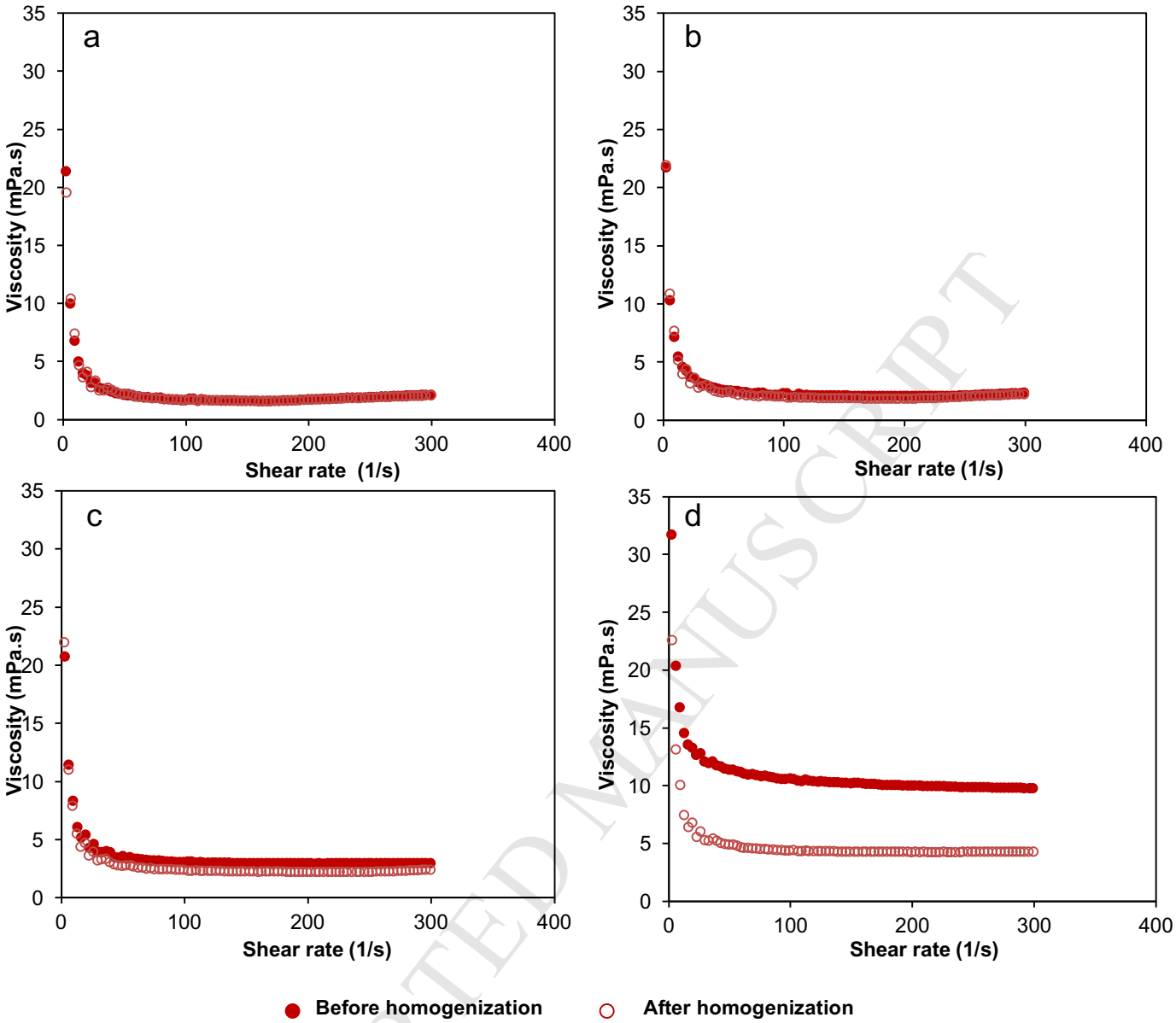

Fig.2

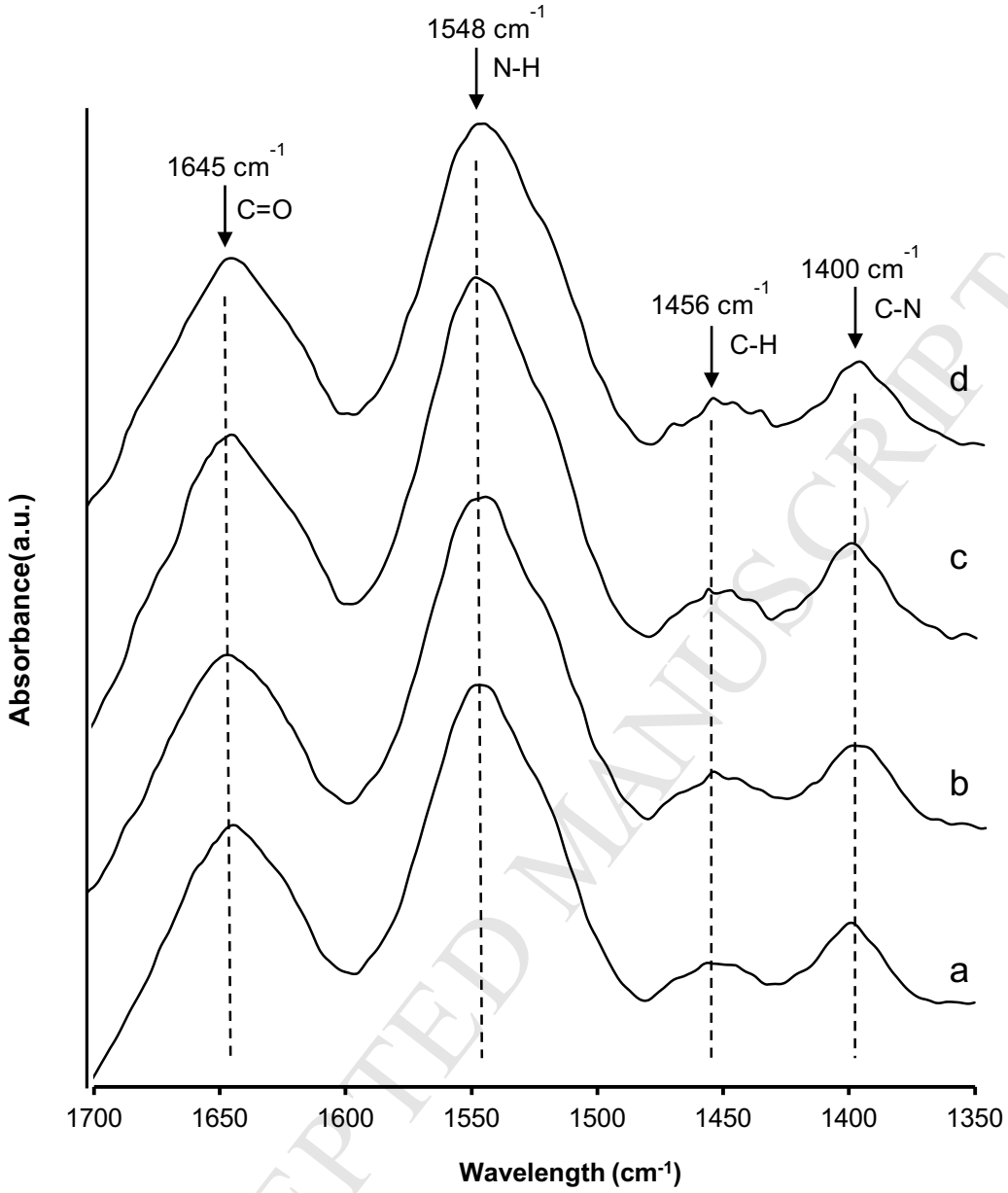

Fig. 3

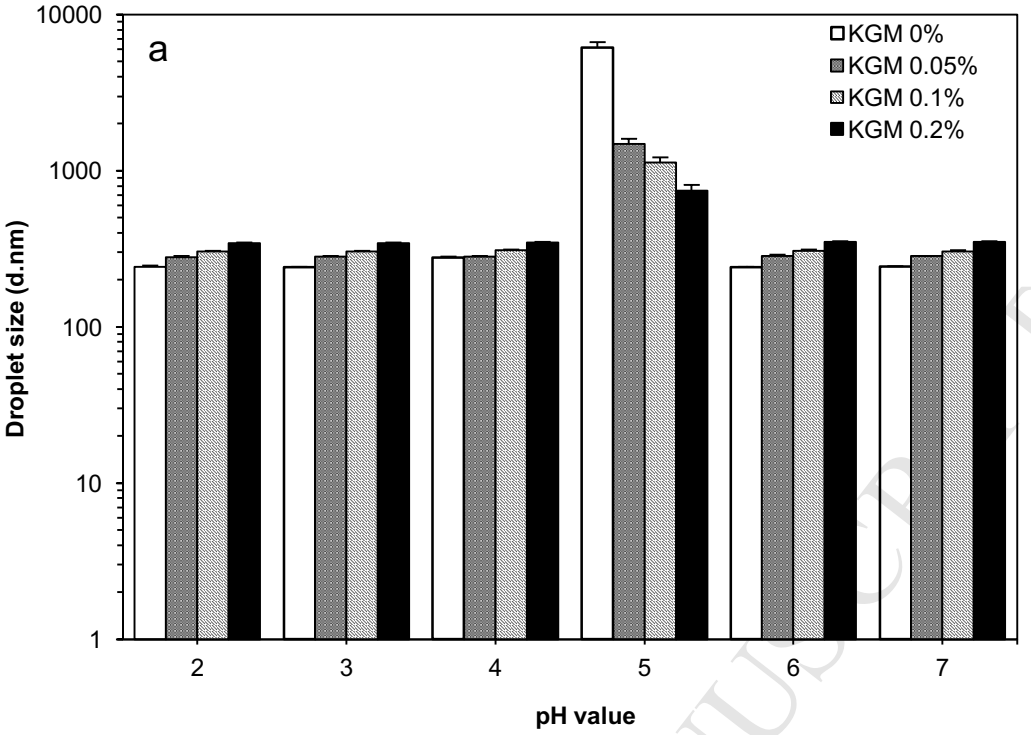

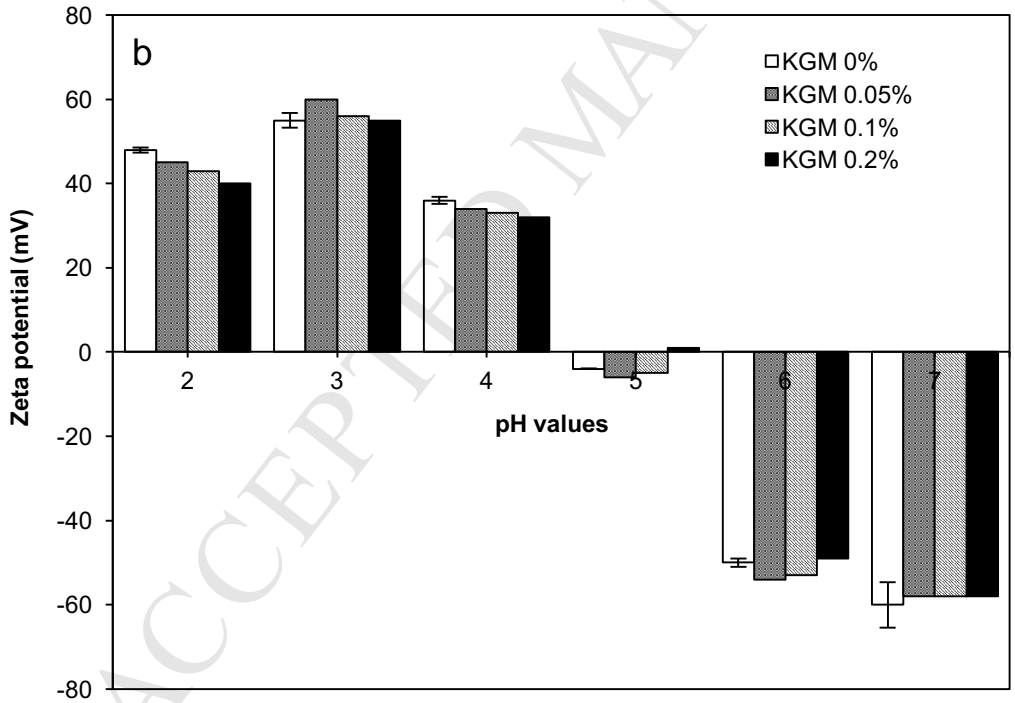

Fig. 4

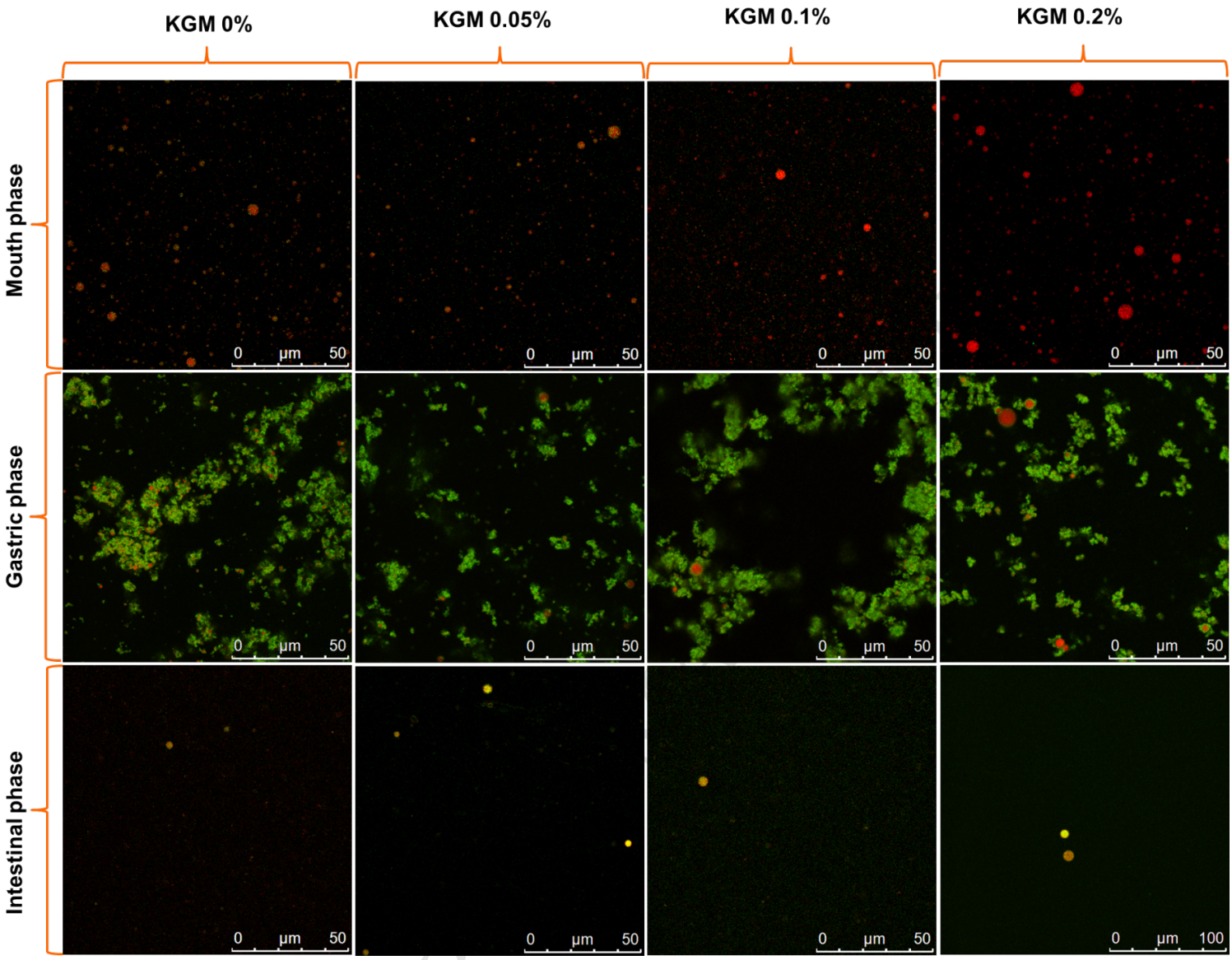

Fig.5

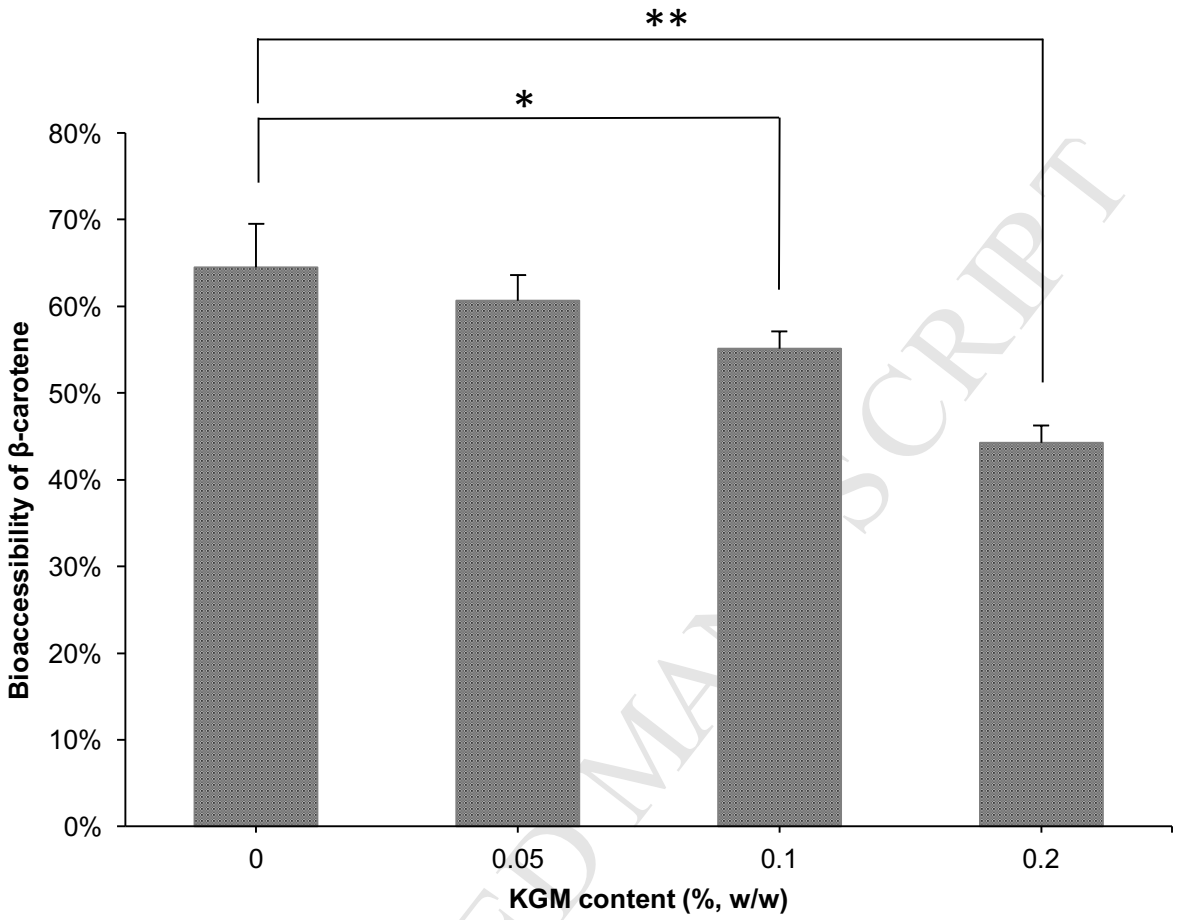

Fig.6

Highlights of this study:

- KGM can significantly improve the stability of WPI-stabilized O/W emulsion
- KGM can significantly decrease the oiling-off of emulsion after freeze-thaw test
- KGM can potentially delay the release of β-carotene from emulsion droplets